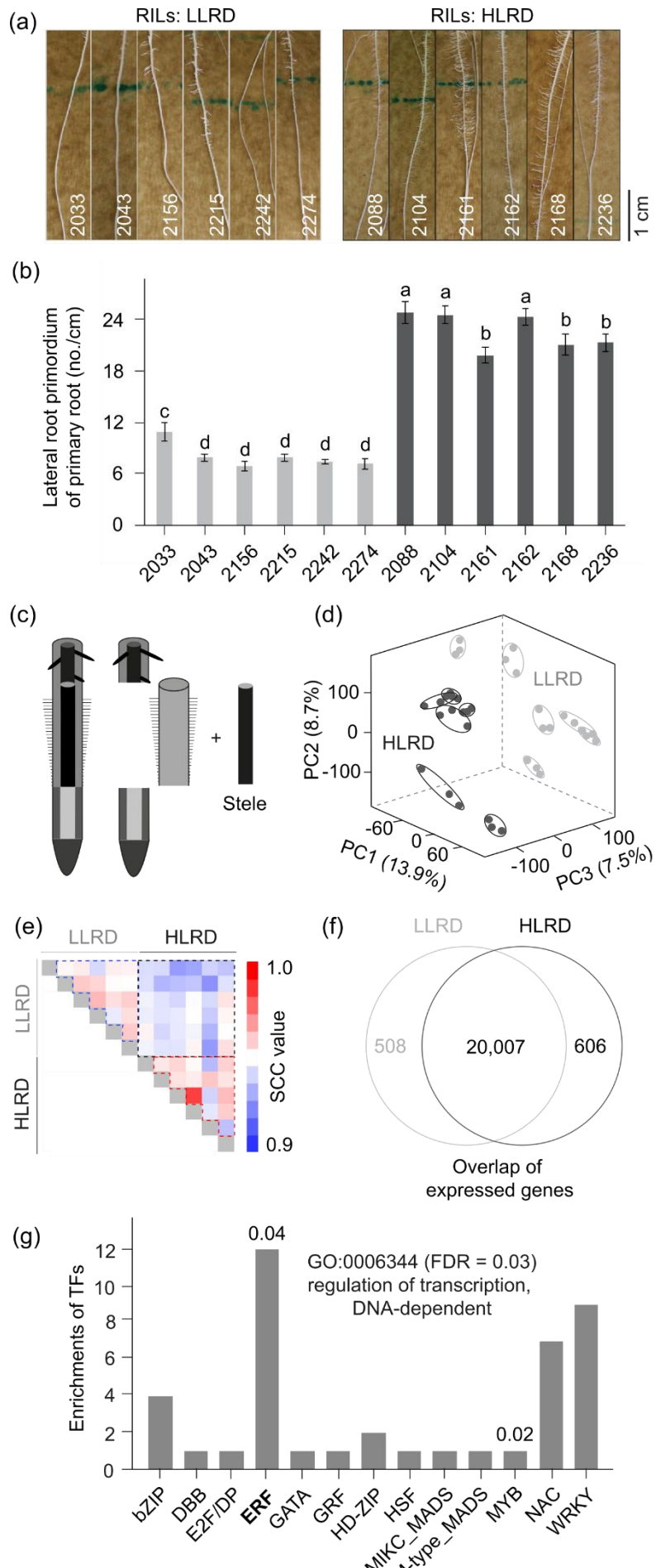


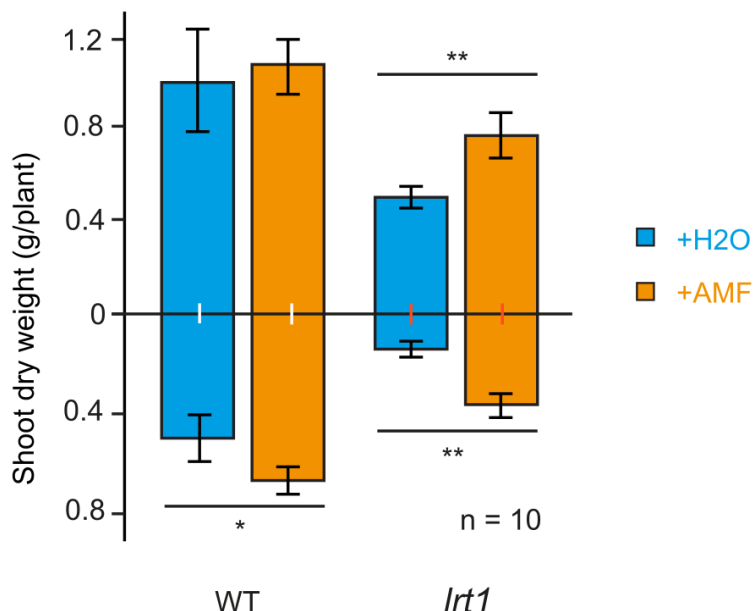
1
2 **Supplementary Figure 1. Weighted gene co-expression network analysis (WGCNA) identifies**
3 **stage- and genotype-specific transcriptional modules associated with pericycle cell competence.**
4 Heatmap showing correlations between module eigengenes (rows, M1–M39) and developmental traits
5 (columns) across pericycle cell types (phloem-pole and xylem-pole), developmental stages (I–III), and
6 genotypes (*lrlt1* mutant and wild type). The color scale indicates Spearman correlation coefficients (SCC)
7 ranging from negative (green) to positive (pink) correlations. Modules exhibiting strong positive
8 correlations (SCC > 0.5) with specific pericycle cell types or developmental stages indicate
9 transcriptional programs tightly associated with cell division competence and lateral root initiation.
10 Notably, modules M8, M9, M11, and M12 are enriched in Stage III phloem-pole pericycle cells of wild-
11 type roots, consistent with their transcriptional activation during pericycle cell transition into actively
12 dividing states. These modules were further analyzed for transcription factor enrichment and motif

13 composition, revealing a predominant role for the ERF gene family in regulating pericycle developmental
14 reprogramming. PPPC, phloem-pole pericycle cell; XPPC, xylem-pole pericycle cell.



16 **Supplementary Figure 2. Transcriptome profiling of stele tissue (comprising pectacycle) from**
 17 **recombinant inbred lines (RILs) differing in lateral root density reveals transcriptional signatures**
 18 **associated with root branching.** (a) RNA-seq was performed on manually dissected stele tissue from
 19 six maize RILs with low lateral root density and six with high lateral root density, selected from the IBM
 20 population. (b) Lateral root primordia phenotype of these six RILs. (c) Schematic illustration of root stele
 21 separation from non-stele tissue. (d) Principal component analysis (PCA) demonstrates a clear
 22 separation of transcriptomes according to lateral root phenotype, with PC1 explaining the majority of
 23 variation between groups. (e) Heatmap illustrates that spearman correlation coefficient (SCC) of gene
 24 expression among these RILs. (f) Venn diagram showing the number of genes exclusively expressed
 25 in high- and low-density RIL groups. A total of 606 genes were specifically expressed in high-density
 26 RILs, while 508 genes were enriched in low-density RILs. (g) GO enrichment analysis of high-density-
 27 specific genes highlights significant overrepresentation of transcriptional regulators, particularly ERF
 28 and MYB transcription factor families (Fisher's exact test $p < 0.05$), suggesting their potential role in
 29 promoting lateral root initiation. FDR, false discovery rate.

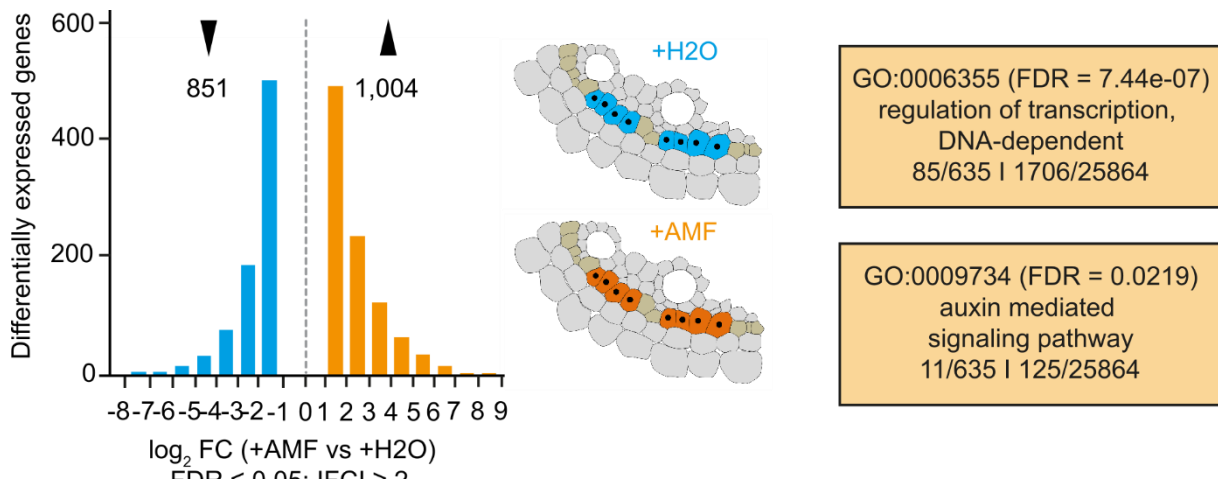
30



31

32 **Supplementary Figure 3. Arbuscular mycorrhizal fungi (AMF) promote shoot biomass in maize**
 33 ***lrt1* mutants under phosphate-poor conditions.**

34 Shoot dry weight was measured in 6-week-old wild type (WT) and *lrt1* mutant plants grown in phosphate-
 35 poor artificial soil, with or without inoculation of arbuscular mycorrhizal fungi (AMF). AMF treatment
 36 significantly increased shoot dry biomass in both WT and *lrt1* plants compared to the water control
 37 (+H₂O). Notably, *lrt1* mutants showed a more pronounced biomass recovery upon AMF inoculation.
 38 Data represent mean \pm SE ($n = 10$ plants per genotype per treatment). Statistical significance was
 39 assessed by two-sided Student's *t*-test: $p < 0.05$ (*), $p < 0.01$ (**).

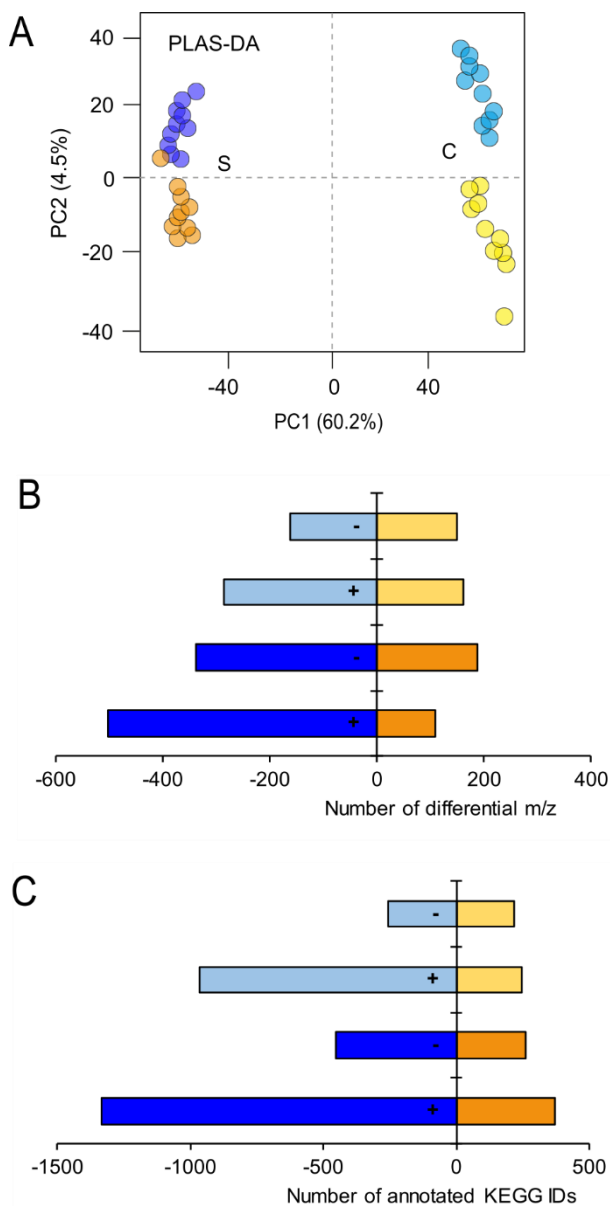


40

41 **Supplementary Figure 4. AM fungi trigger transcriptomic reprogramming in *Irt1* pericycle cells,**

42 enriching transcriptional and auxin signaling pathways.

43 Bar plots display the number of differentially expressed genes (DEGs) in *Irt1* pericycle cells upon AM
 44 fungal inoculation (+AMF, orange) compared to the water control (+H₂O, blue). A total of 1,004 genes
 45 were upregulated and 851 genes were downregulated (|FC| ≥ 2 , FDR ≤ 0.05). Schematics indicate the
 46 sampled phloem-pole pericycle region captured by LCM for transcriptomic profiling. GO enrichment
 47 analysis of upregulated genes in response to AM fungi identified significant overrepresentation of genes
 48 involved in “regulation of transcription, DNA-dependent” (GO:0006355; FDR = 7.44e-07) and “auxin-
 49 mediated signaling pathway” (GO:0009734; FDR = 0.0219), suggesting transcriptional reprogramming
 50 of hormone-responsive networks underlying AMF-induced lateral root development in *Irt1*.

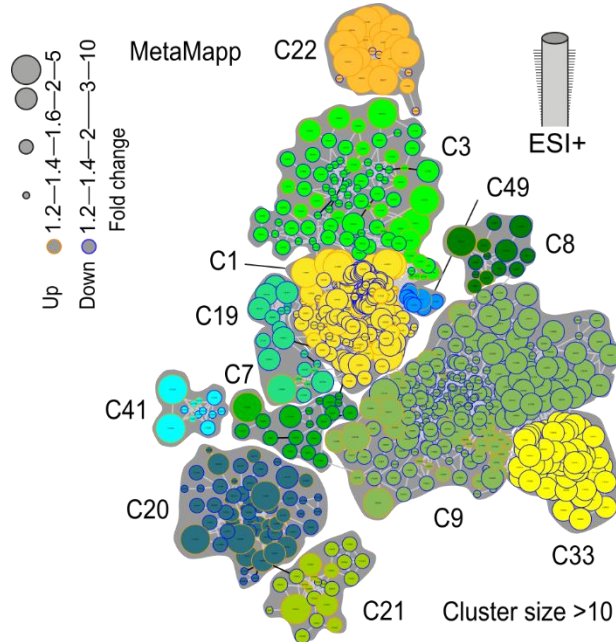


53 **Supplementary Figure 6 Metabolomic reprogramming of *Irt1* roots in response to AM fungal**
 54 **colonization across tissues.**

55 (A) Principal coordinates analysis (PCoA) of metabolite profiles in *Irt1* root cortex and stele tissues
 56 inoculated with or without AM fungi. Each dot represents a distinct metabolic feature (m/z), colored by
 57 tissue and treatment. AMF inoculation induces distinct shifts in metabolic composition, particularly in
 58 cortex tissue.

59 (B) Bar plots showing the number of significantly differentially abundant mass features (m/z) in cortex
 60 (right groups) and stele (left groups) tissues, grouped by treatment (+/- AMF) and tissues (stele vs
 61 cortex). Positive (+) and negative (-) bars indicate upregulated or downregulated m/z features,
 62 respectively.

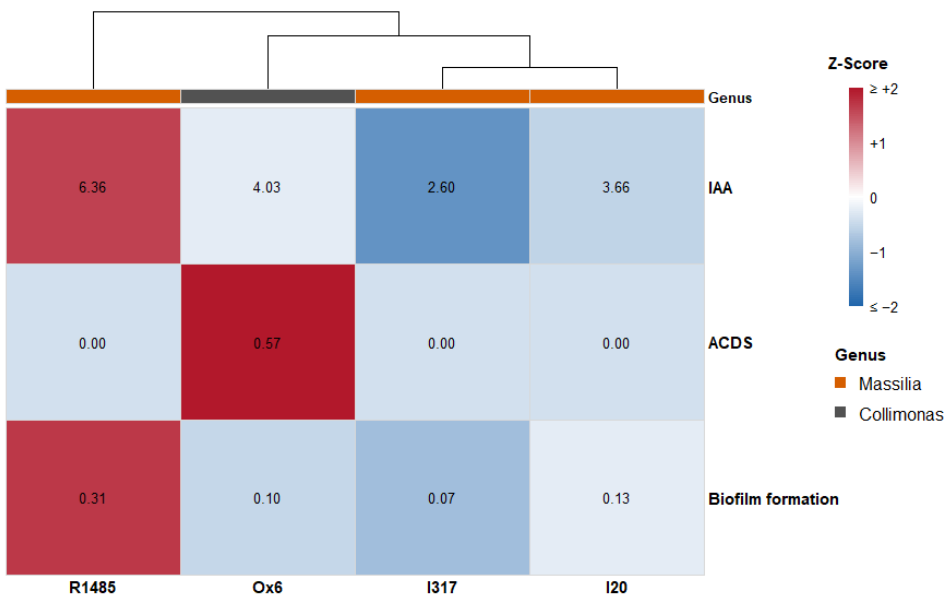
63 (C) Corresponding numbers of differentially annotated KEGG metabolic IDs based on the same
 64 comparisons shown in (B), highlighting AMF-driven reprogramming of known metabolic pathways,
 65 particularly in the cortex tissue.



66

67 **Supplementary Figure 7 Metabolic network of maize root cortex metabolites in response to AM**
 68 **fungal colonization.**

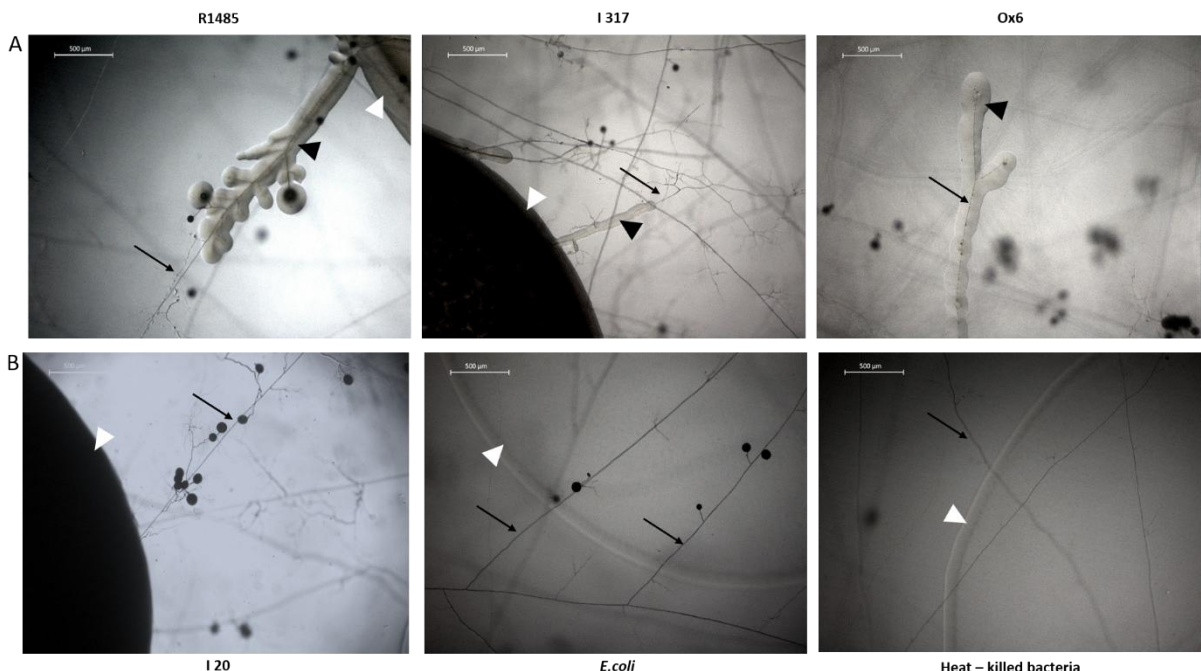
69 The network map was generated using MetaMapp based on chemical similarity and known biochemical
 70 relationships among detected metabolites. Each node represents a unique metabolite detected in the
 71 cortex tissue of *lrl1* mutant roots, and edges connect structurally or biochemically related metabolites.
 72 Node color denotes major chemical classes (e.g., flavonoids in blue/purple, sesquiterpenes in yellow,
 73 amino acid derivatives in green, fatty acids in cyan), while node size reflects the magnitude of fold
 74 change in abundance between AM fungi-inoculated and non-inoculated samples. Only metabolites
 75 significantly altered ($\text{VIP} \geq 1$, $\text{FC} \geq 1.2$ or ≤ 0.8 , $q < 0.05$) are shown.



76

77 **Supplementary Figure 8 Heatmap of plant growth-promoting traits of selected bacterial**
 78 **isolates.**

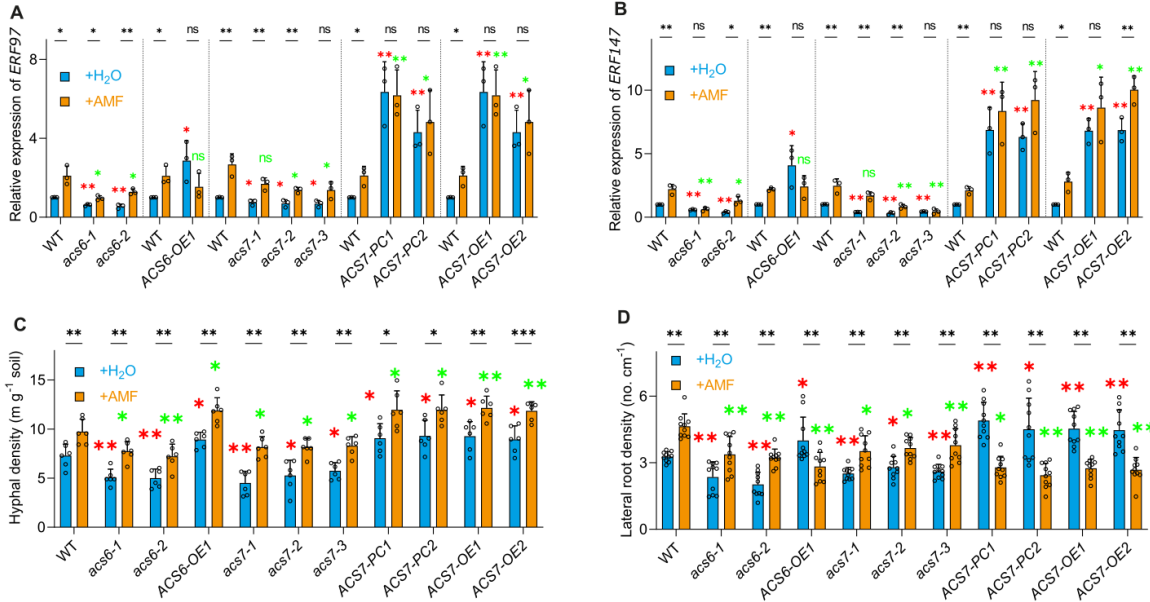
79 Heatmap showing indole-3-acetic acid (IAA) production, ACC deaminase activity (ACDS), and
 80 biofilm formation of the isolates R1485, I317, Ox6, and I20. Colors represent Z-scores
 81 calculated for each trait across all isolates (clipped to ± 2), with blue indicating below-average
 82 and red above-average values. Only the four selected isolates are displayed, while
 83 normalization was performed using the complete dataset. Numbers within the cells indicate
 84 the original measured values. IAA production was quantified using the Salkowski assay, ACC
 85 deaminase activity was assessed by growth on ACC as the sole nitrogen source, and biofilm
 86 formation was determined by crystal violet staining in microtiter plates.



87

88 **Supplementary Figure 9 Light microscopy images showing *Massilia* biofilm formation along AM**
 89 **fungal hyphae.**

90 Images illustrate the frequency and relative intensity of biofilm formation across hyphal
 91 networks. Hyphae are indicated by black arrows, bacterial inoculation spots by white triangles,
 92 free bacteria by blue triangles and bacterial biofilms by black triangles. Scale is 500 μ m.



93
94
95

Supplementary Figure 10 Ethylene biosynthesis via ACS6/ACS7 modulates ERF activation, hyphal proliferation, and lateral root development under AMF colonization.

96 (A, B) Expression levels of *ERF97* (A) and *ERF147* (B) quantified by qRT-PCR in roots of indicated
97 genotypes, with or without AMF inoculation. Both ERF genes are significantly upregulated upon AMF
98 colonization in wild type and overexpression lines, but this induction is impaired in *acs6-1* and *acs7-1*
99 mutants.

100 (C) Hyphal length density (mg g⁻¹ soil) in the rhizosphere. AMF-induced hyphal proliferation is
101 significantly reduced in *acs6-1* and *acs7-1* mutants, but enhanced in overexpression and promoter
102 construct lines, indicating ethylene biosynthesis promotes extraradical hyphal development.

103 (D) Lateral root density (no. cm⁻¹) is increased in WT and ACS-OE/PC lines upon AMF colonization,
104 but not in *acs6-1* or *acs7-1* mutants, showing that ethylene is required for AM-induced root branching.

105 Bars represent mean ± SD (n = 4–6).

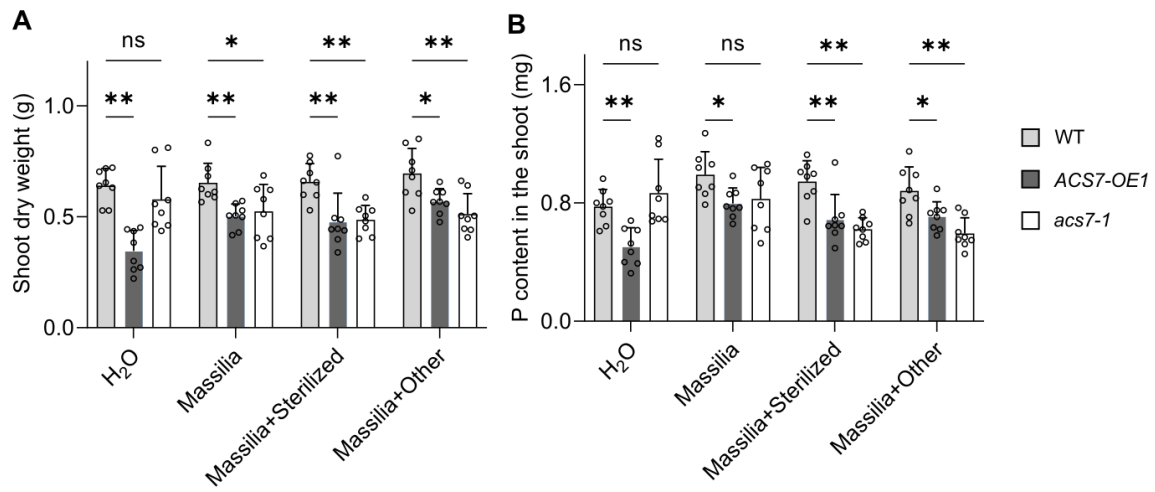
106 Student's t-test was used for pairwise comparisons between treatments.

107 Significance is indicated as:

108 Green asterisks – AMF treatment effect (*P < 0.05, **P < 0.01),

109 Red asterisks – genotype effect,

110 ns – not significant.



111
 112
 113
 114

Supplementary Figure 11 Despite the negative growth and phosphorus acquisition phenotype of ACS7 overexpression, *Massilia* inoculation compensates by restoring both shoot biomass (A) and phosphorus uptake (B).

115 **Supplementary Table 1.** Functional characterization of pericycle cell type specifically enriched modules
 116 (M5, M6, M7, M26, M32 and M33). PPPC, phloem-pole pericycle cell; XPPC, xylem-pole pericycle cell.
 117 FDR, false discovery rate.

Module (M) #	Cell type enriched	Module genes #	Enriched GO (FDR <0.05)	Enriched pathway	Gene ID	Gene name ^a
M5	PPPC	1630	GO: 0022402 (FDR = 0.045)	Cell process cycle	GRMZM2G128938	atr1
					GRMZM2G037926	cki2
					GRMZM2G157510	cki3
					GRMZM2G158526	cenH3
					GRMZM2G333916	met1
					GRMZM5G822970	mmus2
					GRMZM2G173162	msh4
					GRMZM2G033828	rrb3
					GRMZM2G129913	spo1
					GRMZM2G157817	xrcc3
					GRMZM2G395736	-
					GRMZM2G334857	-
					GRMZM2G134694	-
					GRMZM2G472023	-
					GRMZM2G100473	-
					GRMZM2G326328	-
M6	PPPC	275	GO: 0015630 (FDR = 0.048)	Microtubule cytoskeleton	GRMZM2G300709	-
					GRMZM2G025340	-
					GRMZM2G133969	-
					GRMZM2G436981	krp11
					GRMZM2G020216	mpk2
					GRMZM2G104704	-
					GRMZM2G334142	-
M7	PPPC	1900	GO: 0015630 (FDR = 0.00269)	Regulation of mitotic metaphase/anaphase transition	GRMZM2G091543	-
					GRMZM2G471186	-
					GRMZM2G332809	-
					GRMZM2G555108	-
					GRMZM5G899300	bub3
					GRMZM2G047143	mad2
M26	XPPC	1,864	GO: 0009832 (FDR = 0.014)	Plant-type cell wall biogenesis	GRMZM2G022065	-
					GRMZM2G170591	-
					GRMZM2G009913	-
					GRMZM2G112072	-
					GRMZM2G339122	expa1
					GRMZM2G074585	expa3
					GRMZM2G112336	cesa1
					GRMZM2G027723	cesa2
					GRMZM2G424832	cesa4
					GRMZM2G070360	dba2
					GRMZM2G073725	gap1
					GRMZM2G013324	gpx11
					GRMZM2G026218	mmp18 7
					GRMZM2G069047	nactf11 5
					GRMZM2G102946	rop5
					GRMZM5G898668	xt5
					GRMZM2G135743	-
					GRMZM5G804575	-
					GRMZM2G076394	-
					GRMZM2G007953	-

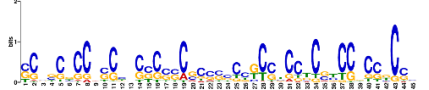
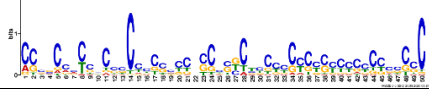
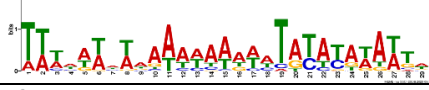
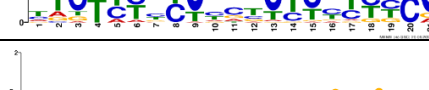
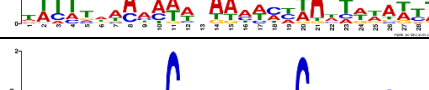
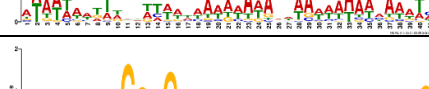
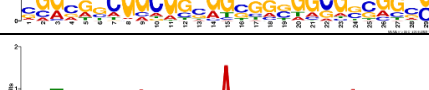
					GRMZM2G030167	-
					GRMZM2G001079	-
					GRMZM2G020721	-
					AC233901.1_FG008	-
M32	XPPC	131	GO: 0009755 (FDR = 0.024)	hormone-mediated signaling pathway	GRMZM2G104176	iaa7
					GRMZM2G031615	iaa14
					GRMZM2G180328	nactf20
					GRMZM2G137046	bzip61
					GRMZM2G042429	-
					GRMZM2G145518	-
					GRMZM2G001799	iaa41
M33	XPPC	268	GO: 0009734 (FDR = 0.014)	auxin mediated signaling pathway	GRMZM5G825707	iaa6
					GRMZM2G074267	pin2
					GRMZM2G061515	aas6
					GRMZM2G002515	bri2
					GRMZM2G378580	arftf13
					GRMZM2G012636	-

118

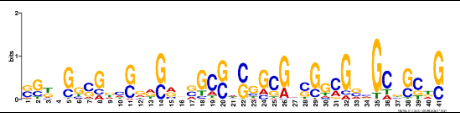
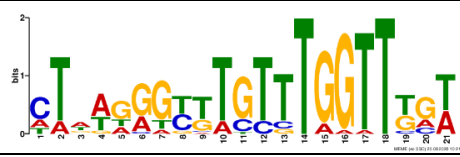
119 ^a gene name in maize GDB.

120
121
122

Supplementary Table 2. MEME enriched motifs within 1 kb upstream and 0.5 kb downstream of promoter region of the pericycle cell division (stage 3) specifically enriched module (M9, M11, M12) genes.

Module (M) #	Motif #	E-value	Sites	Width	Sequence logo
M9	1	1.0e-089	97	45	
	2	6.8e-061	96	29	
	3	1.3e-077	86	50	
	4	4.9e-043	62	29	
	5	5.9e-035	75	29	
	6	7.0e-028	88	20	
	7	6.6e-016	102	21	
	8	1.0e-018	93	28	
	9	5.1e-010	106	29	
	10	2.7e-008	57	29	
M11	1	9.8e-084	79	29	
	2	1.2e-081	91	41	
	3	4.5e-080	83	29	
	4	2.1e-033	58	29	

M12	5	4.4e-026	61	21	
	6	5.3e-039	88	37	
	7	2.1e-015	56	15	
	8	1.9e-014	60	29	
	9	4.6e-007	68	21	
	10	2.6e-006	28	21	
	1	4.9e-104	143	29	
	2	1.0e-098	107	29	
	3	9.0e-067	87	41	
	4	6.9e-046	157	21	

	9	2.5e-028	70	41	
123	10	6.4e-006	23	21	

124 **Supplementary Table 3.** TOMTOM identified top twenty *cis*-motifs with the most significant matches to
 125 the ERF transcription factors using JASPAR CORE Plants database. TF, transcription factor.

Module (M) #	Input Motif #	Total matches	Significant matches (<i>q</i> - value < 0.05)	AP2/ERF domain Class	Matching TF ^a	<i>q</i> -value
M9	1	55	38	36	ERF104	2.44e-03
	4	64	54	52	ERF9	4.33e-07
	8	48	32	32	ERF3	1.06e-02
	10	71	51	50	ERF4	8.05e-04
M11	3	61	54	54	ERF9	1.25e-07
	5	56	27	26	ERF104	5.22e-3
	6	48	11	10	CRF4	8.16e-03
	8	52	4	4	ERF4	2.97e-02
M12	1	59	54	54	ERF9	2.77e-08
	5	64	44	41	CRF2	7.39e-04
	7	59	30	30	ERF104	9.40e-03
	9	63	46	46	ERF104	2.02e-3

126
 127 ^a Transcription factors of which the known binding motif most significantly matches the identified motif
 128 (*q*-value < 0.05) in *Arabidopsis*.

129 **Supplementary Table 4.** Functional characterization of proteins exhibiting stele-specific enrichment in
130 response to AM fungi inoculation. "+" enriched in response to AM fungi; "-" depleted in response to AM
131 fungi.

Protein ID	KEGG	Description	GO (Biological Process)	Enrichment
tr A0A1D6NEY9 A0A1D6NEY9_MAIZE	K00799	glutathione S-transferase	GO:0048527, lateral root development	0.74 (-)
tr K7TXJ3 K7TXJ3_MAIZE	K01807	ribose 5-phosphate isomerase A	GO:0055085, transmembrane transport	0.12 (-)
tr Q9M588 Q9M588_MAIZE	K17080	prohibitin 1	GO:0048527, lateral root development	0.8 (-)
tr B4FIE9 B4FIE9_MAIZE	K00789	S-adenosylmethionine synthetase	GO:0006556, S-adenosylmethionine biosynthetic process	1.3 (+)
tr B6SIK2 B6SIK2_MAIZE	/	/	/	1.51 (+)
tr B4FVJ0 B4FVJ0_MAIZE	K02930	large subunit ribosomal protein L4e	GO:0006412, translation	1.24 (+)
tr B6SJ21 B6SJ21_MAIZE	K14753	guanine nucleotide-binding protein subunit beta-2-like 1 protein	GO:0048364, root development	1.28 (+)

132

133 **Supplementary Table 5.** Proteins exhibiting enrichment in cortex tissue in response to AM fungi
 134 inoculation are annotated to Phenylpropanoid biosynthesis. "+" enriched in response to AM fungi; "-"
 135 depleted in response to AM fungi.

Protein ID	Description	Enrichment	Coding gene ID
tr B6TBU1 B6TBU1_MAIZE	1-aminocyclopropane-1-carboxylate oxidase	1.52 (+)	AC148152.3_FG005
sp P49235 HGGL1_MAIZE	4-hydroxy-7-methoxy-3-oxo-3,4-dihydro-2H-1,4-benzoxazin-2-yl glucoside beta-D-glucosidase 1, chloroplastic	1.41 (+)	GRMZM2G016890
tr A0A1D6EZ64 A0A1D6EZ64_MAIZE	Polygalacturonase inhibitor 1	1.47 (+)	GRMZM2G099295
tr A0A1D6HY96 A0A1D6HY96_MAIZE	Serine carboxypeptidase-like 19	1.4 (+)	GRMZM2G471269
tr A0A1D6MUP9 A0A1D6MUP9_MAIZE	Beta-glucosidase 17	1.34 (+)	GRMZM2G426467
tr A0A1D6IXD5 A0A1D6IXD5_MAIZE	Beta-glucosidase2	1.43 (+)	GRMZM2G008247
tr A0A1D6GWL6 A0A1D6GWL6_MAIZE	GDSL esterase/lipase	1.39 (+)	GRMZM2G132331
tr B4FHG3 B4FHG3_MAIZE	Peroxidase	1.33 (+)	GRMZM2G108219
tr A0A1D6E530 A0A1D6E530_MAIZE	Peroxidase	1.34 (+)	GRMZM2G108153
tr C0HHA6 C0HHA6_MAIZE	Peroxidase	1.34 (+)	GRMZM2G122853
tr B6T3V1 B6T3V1_MAIZE	Peroxidase	1.37 (+)	GRMZM2G089982
tr C4J6E4 C4J6E4_MAIZE	Peroxidase	1.39 (+)	GRMZM2G126261
tr B6SIU4 B6SIU4_MAIZE	Peroxidase	1.43 (+)	GRMZM2G144648
tr A0A1D6F4C8 A0A1D6F4C8_MAIZE	Peroxidase	1.46 (+)	GRMZM2G133475
tr A0A1D6LYW3 A0A1D6LYW3_MAIZE	Peroxidase	1.56 (+)	GRMZM2G135108
tr D7NLB3 D7NLB3_MAIZE	Peroxidase	1.62 (+)	GRMZM2G410175
tr B4FG39 B4FG39_MAIZE	Peroxidase	1.67 (+)	GRMZM2G108123
tr A0A1D6KAW3 A0A1D6KAW3_MAIZE	Peroxidase	1.73 (+)	GRMZM2G088765
sp Q9FEQ8 PER2_MAIZE	Peroxidase 2	1.71 (+)	GRMZM2G040638
tr A0A1D6HDL5 A0A1D6HDL5_MAIZE	Phenylalanine ammonia-lyase	0.74 (-)	GRMZM2G029048

Supplementary Table 6. Primers used for gene cloning, expression, and vector construction

Gene	Primer (5' to 3')	Accession #
ZmACS6_qF	GGCAGCATCATTAGCAGTAGGA	
ZmACS6_qR	ACCACTCCTGCTCCTACCTAAT	GRMZM2G054361/Zm00001d03386
ZmACS6-CRISPR-F	TGGGGTGGGAGGGAGTATGA	2
ZmACS6-CRISPR-R	GTATGGCGTGGGGATGAGA	
ZmACS7_qF	CGTACGTAGCTAGCTTGACATT	
ZmACS7_qR	TTGACTAGCTGCTTACCGCC	
ZmACS7-CRISPR-F	AGCAAGCTCATGCCCTCAA	
ZmACS7-CRISPR-R	AGCATTGGACTTGGATCGGC	GRMZM5G894619/Zm00001d02606
ZmACS7-PC-F	AGGGTGAAGCTAACGTGTC	0
ZmACS7-PC-R	TGTCACTCTGTGTAATGTCAAG	
ZmERF1_qF	GGCTTCGAACTGGATCTGAAC	5
ZmERF1_qR	GCCATACAGGACCAAAACAACC	
ZmERF2_qF	TCGATCGTTAATTGCCCTGCC	GRMZM2G068967/Zm00001d00236
ZmERF2_qR	TGTTTATACCACGTAGCCTGCC	4
C2_qF	CTGGCCTCATCTCCAAGAACAT	
C2_qR	CATCTCGTCGAGGATGAAGAG	GRMZM2G422750/Zm00001d05267
qZmTublinF	GCTATCCTGTGATCTGCCCTGA	3
qZmTublinR	CGCCAAACTTAATAACCCAGTA	GRMZM2G152466/Zm00001d01336
F1048	GTGSTGCAYGGYTGTCGTCA	7
R1194	ACGTCRTCCMCACCTTCCTC	
qRT_Massilia_FW	GGAGCGGCCGATRTCTGATTA	
qRT_Massilia_RV	G	
	ATTCTACCCCCCTCTGCCARAY	